From Molecular Property to Catalytic Mechanism: A DFT Study on the Formation of High-Density cis-syn-cis-Perhydrophenanthrene

Shaofei Zhang[ab], Wannan Wang[ab], Zhigang Fan[ab], Zewen Fan[ab], Jing Ren[b], Rui-Peng Ren[ab]*, Yong-Kang Lv[ab]*

[a] State Key Laboratory of Clean and Efficient Coal Utilization, Taiyuan University of Technology, Taiyuan 030024, Shanxi, China

[b] College of Chemistry and Chemical Engineering, Taiyuan University of Technology, Taiyuan 030024, Shanxi, China

Email: renruipeng@tyut.edu.cn (Rui-Peng Ren); lykang@tyut.edu.cn (Yong-Kang Lv)

1. Physical property calculation

1.1. Calculation for density

Density is of paramount importance for high energy density fuels (HEDFs), as a higher density means a fuel tank of fixed volume can carry a greater mass of fuel, which significantly enhances the range, payload, and speed of aerospace vehicles. Using multiple molecular dynamics (MD) simulations to determine density can yield results closer to experimental values, while DFT method offers higher computational efficiency compared to MD simulations. Therefore, we combined DFT and MD methods for the isomer screening of PHP.

DFT method

Density was calculated using the DFT method via Equation (1) [1, 2].

$$\rho = \alpha\left(\frac{M}{0.001\,V}\right) + \beta\nu\left(\sigma_{\text{tot}}^2\right) + \gamma \tag{1}$$

The density estimated by the relative molecular mass (M) and the van der Waals volume (V_m) of the molecule is given by M/V, where V_m represents the volume of an isolated gas-phase molecule in cm^3/molecule. Following the proposal of Bader et al. , this volume is defined as the space enclosed by the 0.001 au ($e/Bohr^3$) isosurface of the

molecular electron density (r) [3]. The term $v\sigma 2$ tot accounts for electrostatic interactions, where v denotes the balance degree of positive and negative charges on the isosurface, and $\sigma 2$ tot measures the potential variation on the molecular surface. Three fitting coefficients (α=0.9183, β=0.0028, γ=0.0443) were used to correlate with experimental data. The parameters V_m, v, and $\sigma 2$ tot of fuel molecules were obtained using the Multiwfn 3.8 software [4, 5].

MD simulations

MD simulations were performed using the LAMMPS package[6], with the COMPASS force field employed throughout all simulations. The COMPASS force field is well-suited for modeling various organic molecules, including alkanes, benzene, and their derivatives, and can accurately predict physical properties such as density and viscosity compared to other force fields [7-10]. First, 128 fuel molecules were dispersed in a simulation box of approximately 30 Å × 30 Å × 30 Å. Geometric optimization and annealing processes were then conducted to obtain stable configurations. During MD simulations, the NPT ensemble was applied under constant temperature (298.15 K) and pressure (1 bar) conditions for a total simulation time of 5 ns, with a time step of 1 fs.

1.2. Calculation of mass net heat of combustion

The mass net heat of combustion refers to the heat released per unit mass of fuel during complete combustion, where water vapor in the combustion products remains in gaseous form. This parameter serves as a critical indicator for evaluating the energy release of high-density fuels in practical combustion processes. The mass net heat of combustion ΔH_c(M) (kJ/g) can be obtained by calculating the combustion enthalpy and evaporation enthalpy per unit mass according to the definition, as shown in Equation (2).

$$\Delta H_c(M) = \frac{\Delta H_c(298.15\ \mathrm{K})(g) + \Delta H_{vap}}{M} \tag{2}$$

Combustion enthalpy is calculated by Equation (3).

$$C_nH_m(g) + \frac{n+m}{2}O_2(g) \rightarrow nCO_2(g) + \frac{m}{2}H_2O(l)$$

$$H_c(298.15\ \mathrm{K})(\mathrm{g}) \rightarrow \Delta E_0 + \Delta ZPE + \Delta H(298.15\ \mathrm{K}) \quad (3)$$

where ΔE_0 represents the electronic energy at 298.15 K and 1 atm, ΔZPE denotes the zero-point energy correction under the same conditions, ΔH(298.15 K) refers to the enthalpy correction term. The *ZPE* and *H*(298.15 K) values for each species were computed using the Shermo software package [11].

Vaporization enthalpy is calculated by Equation (4).

$$\mathrm{C_nH_m(l)} \rightarrow \mathrm{C_nH_m(g)}$$

$$\Delta H_{\mathrm{vap}} = a(SA)^{0.5} + b(v\sigma_{\mathrm{tot}}^2)^{0.5} + c \quad (4)$$

where the surface area of the fuel molecule (*SA*) was obtained using Multiwfn 3.8 software. The fitting coefficients for the enthalpy of vaporization are $a = 2.13$, $b = 0.93$, and $c = -17.84$, respectively.

Mass net heat of combustion is calculated by Equation (5).

$$NHOC(M) = \frac{\Delta H_c}{M} \quad (5)$$

Volume net heat of combustion can be obtained from the mass net heat of combustion, as shown in Equation (6).

$$NHOC(V) = NHOC(M) \times \rho \quad (6)$$

1.3 Calculation for specific impulse

The specific heat of combustion of hydrocarbons, *h* (J/g), is given by:

$$h = 1000 NHOC(M) \quad (7)$$

When polycyclic alkanes react with oxygen at the stoichiometric ratio, the conversion relationship between the specific heat of combustion of the hydrocarbon (*h*) and that of the fuel (hydrocarbon + oxygen) (*H*) is:

$$H = \frac{h(11.91 + x)}{43.66 + 8.93x} \quad (8)$$

where *x* is the ratio of the number of hydrogen to carbon atoms in the fuel molecule.

The formula for specific impulse is [12]:

$$I_{sp} = \frac{(2\eta H)^{0.5}}{g} \tag{9}$$

where the efficiency factor η is 0.556, applicable to most polycyclic alkanes, and the calculated results are in good agreement with experimental values.

1.4. Other properties

Melting point, boiling point, critical temperature, critical pressure, critical volume, flash point, and other properties were estimated using the group contribution method to improve the prediction of the physical properties of PHP [13].

The group contribution method addresses the need for rapid estimation of physical and thermodynamic properties of compounds in chemical engineering and related fields. Its fundamental principle is to treat the properties of a compound as the sum of contributions from each structural group within its molecular architecture. Despite its utility, the group contribution method has limitations regarding the spatial structure of fuel molecules. The influence of spatial structure on fuel properties is well-established, particularly for stereoisomers with distinct stereochemical configurations. A typical example is the difference in freezing points between endo-tetrahydrodicyclopentadiene (endo-THDCPD) and exo-tetrahydrodicyclopentadiene (exo-THDCPD), which arises primarily from the impact of molecular spatial geometry on physical properties. However, the group contribution method cannot capture structural disparities between molecules.

Melting point is calculated by Equation (10).

$$\exp\left(\frac{T_m}{147.45}\right) = \sum_i n_i G_i \tag{10}$$

Boiling point is calculated by Equation (11).

$$\exp\left(\frac{T_b}{222.543}\right) = \sum_i n_i G_i \tag{11}$$

Critical temperature is calculated by Equation (12).

$$\exp\left(\frac{T_c}{231.5239}\right) = \sum_i n_i G_i \tag{12}$$

Calculation of critical Pressure is calculated by Equation (13).

$$(P_c - 5.9827)^{-0.5} - 0.108998 = \sum_i n_i G_i \tag{13}$$

Critical Volume is calculated by Equation (14).

$$V_c - 7.95 = \sum_i n_i G_i \tag{14}$$

G_i represents the contribution of a certain group to the physical property, and the G_i values used are shown in Table S1.

Table S1. G_i values in group contribution method [13].

Groups	G_i				
	T_m	T_b	T_c	P_c	V_c
CH_2(cyclic)	0.5699	0.8234	1.8815	0.009884	49.24
CH(cyclic)	0.0335	0.5946	1.102	0.007596	44.95
CH(multiring)	0.6647	0.1415	1.2513	−3.33	−2.095

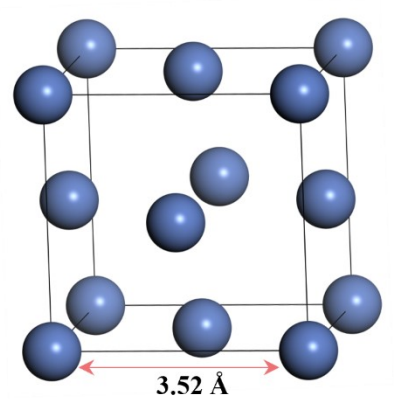

Figure S1. Optimized unit cell of Ni.

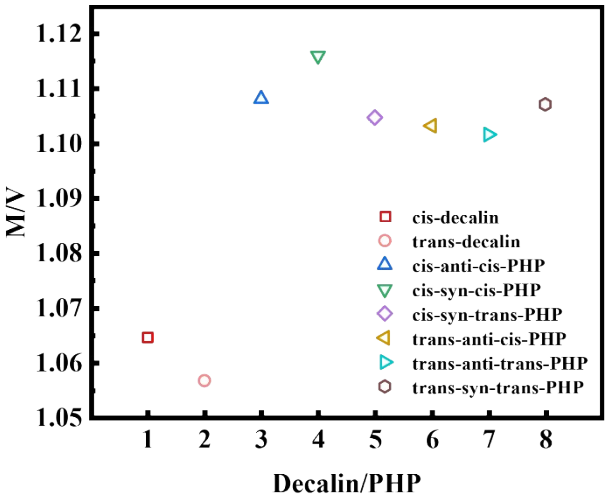

Figure S2. *M*/*V* values for decalin and PHP.

Table S2. Six stable adsorption sites of PHE on the Ni(100) surface.

Site	hhb	**hhh**	bbh
E_{ads}(eV)	−5.03	**−5.26**	−4.90
Top view	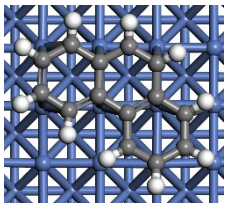	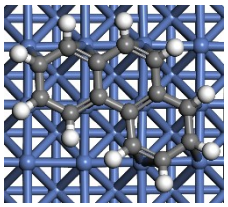	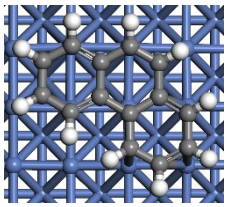
Side view	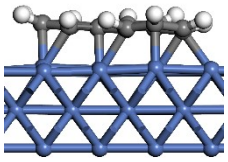	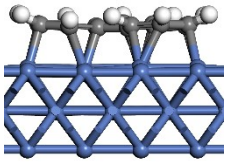	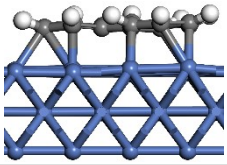

Site	bhb	bbb	hbh
E_{ads}(eV)	−4.52	−3.88	−4.99
Top view	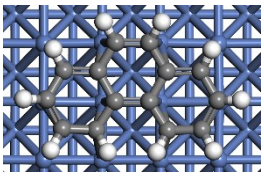	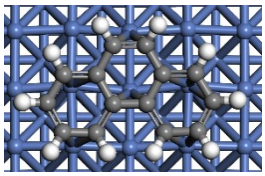	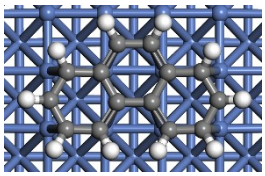
Side view	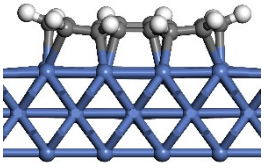	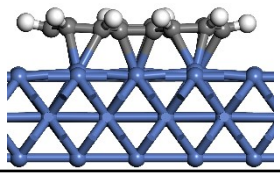	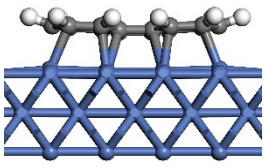

Table S3. Two stable adsorption sites of PHE on the Ni(111) surface.

Site	**b1**	b2
E_{ads}(eV)	**−4.06**	−3.98
Top view	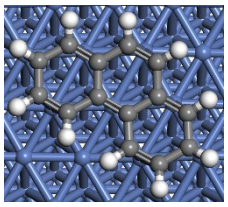	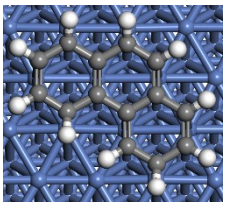
Side view	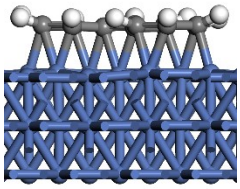	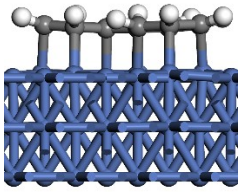

Table S4. Adsorption configurations of three PHE2H intermediates (9,10-A-PHE2H, 9,11-A-PHE2H, 9,12-A-PHE2H) on Ni(100) and Ni(111) surfaces.

	9,10-A-PHE2H	9,11-A-PHE2H	9,12-A-PHE2H
A-PHE2H	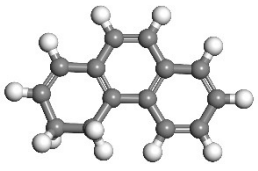	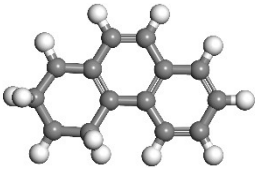	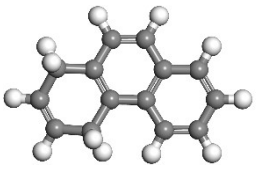
Ni(100)	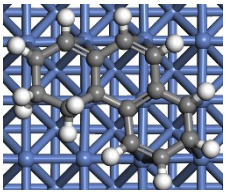	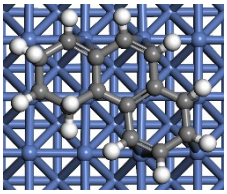	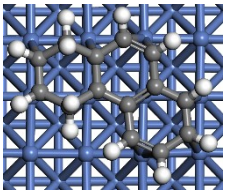
E_{ads}(eV)	−4.86	−6.67	−4.68
Ni(111)	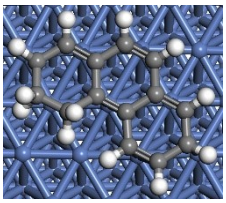	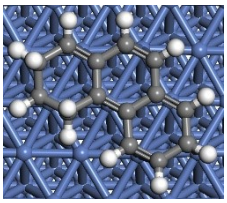	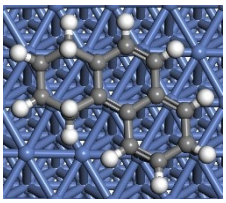
E_{ads}(eV)	−3.83	−5.73	−3.78

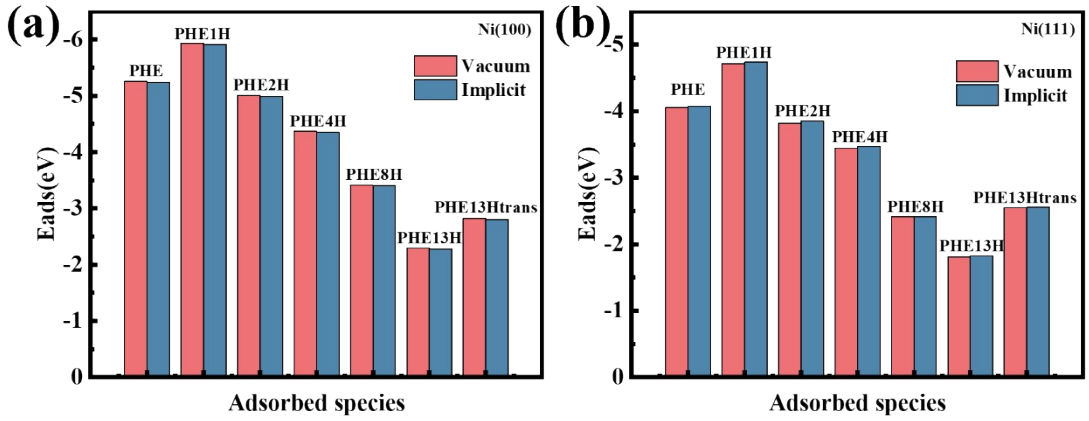

Figure S3. Adsorption energies of PHE and related species in vacuum and decalin solvent on the (a) Ni(100) and (b) Ni(111) surfaces

Table S5 The energy barrier for the first hydrogen addition of PHE on Ni(100) and Ni(111) surfaces.

C atom	Ni(100)	Ni(111)
	E_a(eV)	E_a(eV)
1	0.84	0.73
3	0.87	0.88
4	0.88	0.91
5	0.90	0.88
6	0.80	0.72
9	**0.74**	**0.71**
10	0.95	0.90
11	0.87	0.94
12	0.83	1.05
14	0.86	0.77

Table S6. Energy barriers for the hydrogenation of the A-PHE4H intermediate on Ni(100) and Ni(111) surfaces to form PHE5H.

C atom	Ni(100)	Ni(111)
	E_a(eV)	E_a(eV)
1	0.80	0.70
3	**0.78**	0.98
4	0.93	0.86
5	0.92	0.88
6	0.86	0.77
8	1.06	**0.62**
13	1.00	0.99
14	0.94	0.69

Table S7. Energy barriers for hydrogenation of AC-PHE8H intermediate to AC-PHE9H on Ni(100) surface.

C atom	E_a(eV)
1	0.83
8	**0.73**
13	0.98
14	0.92

Table S8. Energy barriers for hydrogenation of AB-PHE8H intermediate to AB-PHE9H on Ni(111) surface.

C atom	E_a(eV)
2	0.79
3	1.04
4	0.84
5	**0.73**
6	0.89
7	1.05

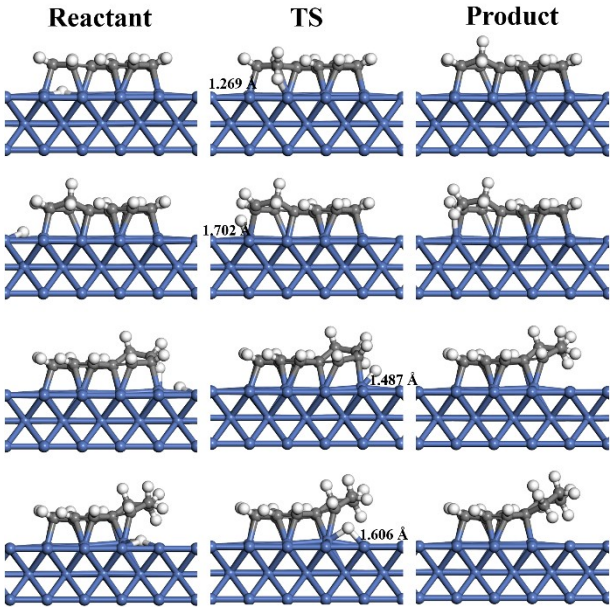

Figure S4. Optimized reactant, transition state, and product structures for the first-ring hydrogenation reaction of PHE on the Ni(100) surface. The first row: 9C+1H; the second row: 10C+2H; the third row: 11C+3H; the fourth row: 12C+4H. The numbers in the figure indicate the C–H bond distances at the transition state.

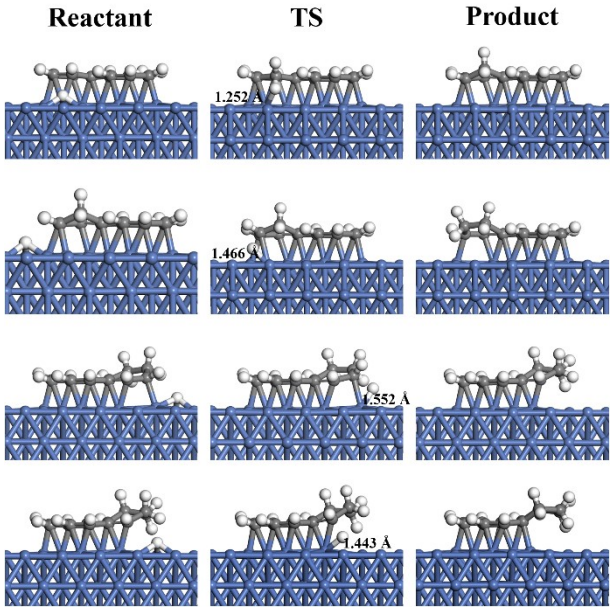

Figure S5. Optimized reactant, transition state, and product structures for the first-ring hydrogenation reaction of PHE on the Ni(111) surface. The first row: 9C+1H; the second row: 10C+2H; the third row: 11C+3H; the fourth row: 12C+4H.

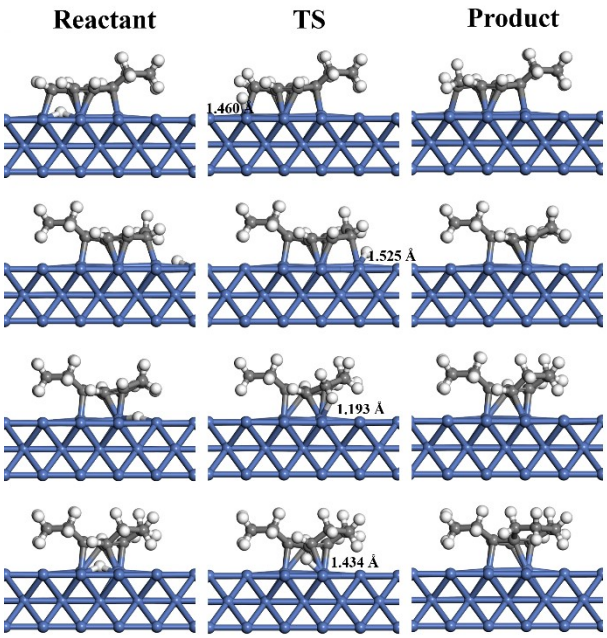

Figure S6. Optimized reactant, transition state, and product structures for the C-aromatic-ring hydrogenation reaction of PHE on the Ni(100) surface. The first row: 3C+1H; the second row: 4C+2H; the third row: 5C+3H; the fourth row: 6C+4H.

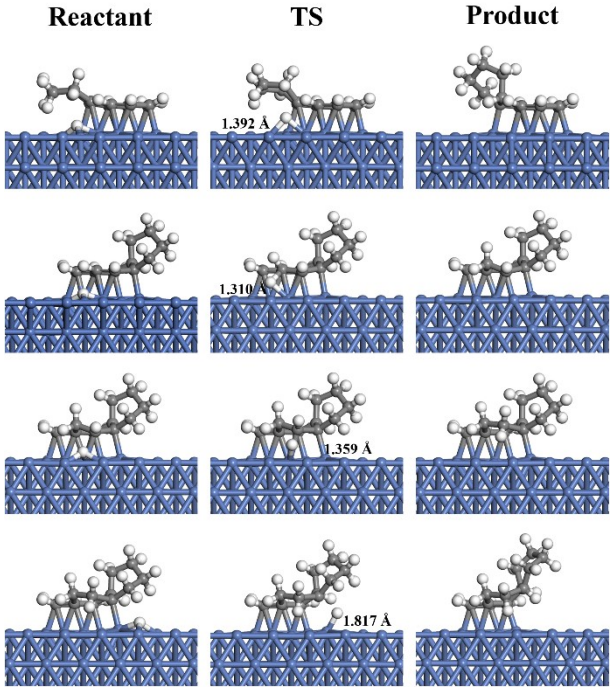

Figure S7. Optimized reactant, transition state, and product structures for the B-aromatic-ring hydrogenation reaction of PHE on the Ni(111) surface. The first row: 8C+1H; the second row: 1C+2H; the third row: 14C+3H; the fourth row: 13C+4H.

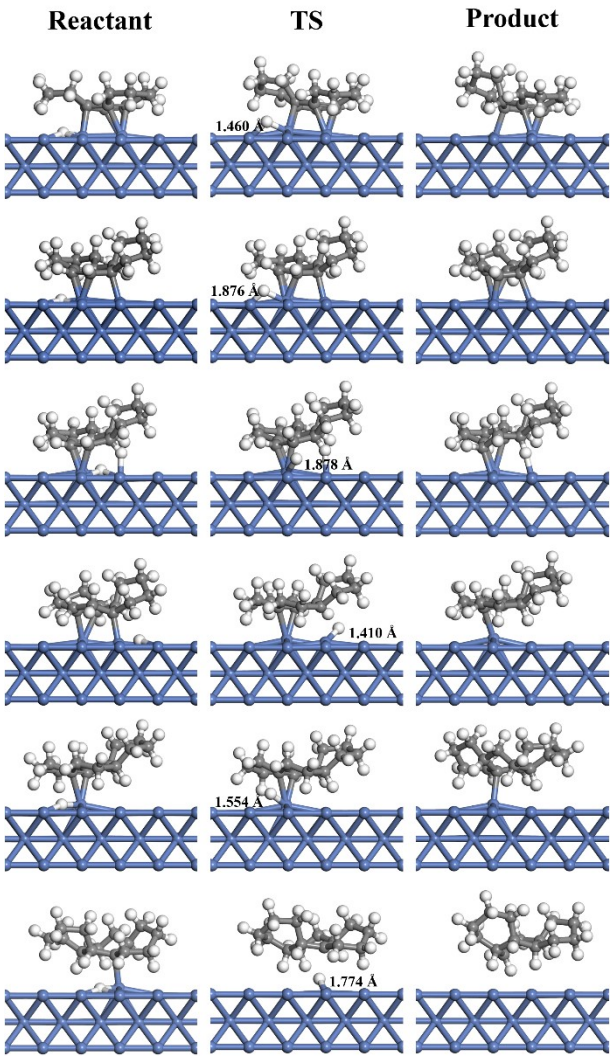

Figure S8. Optimized reactant, transition state, and product structures for the last- aromatic ring hydrogenation reaction of PHE on the Ni(100) surface. The first row: 9C+1H; the second row: 10C+2H; the third row: 11C+3H; the fourth row: 12C+4H; the fifth row: 2C+5H; the sixth row: 7C+6H.

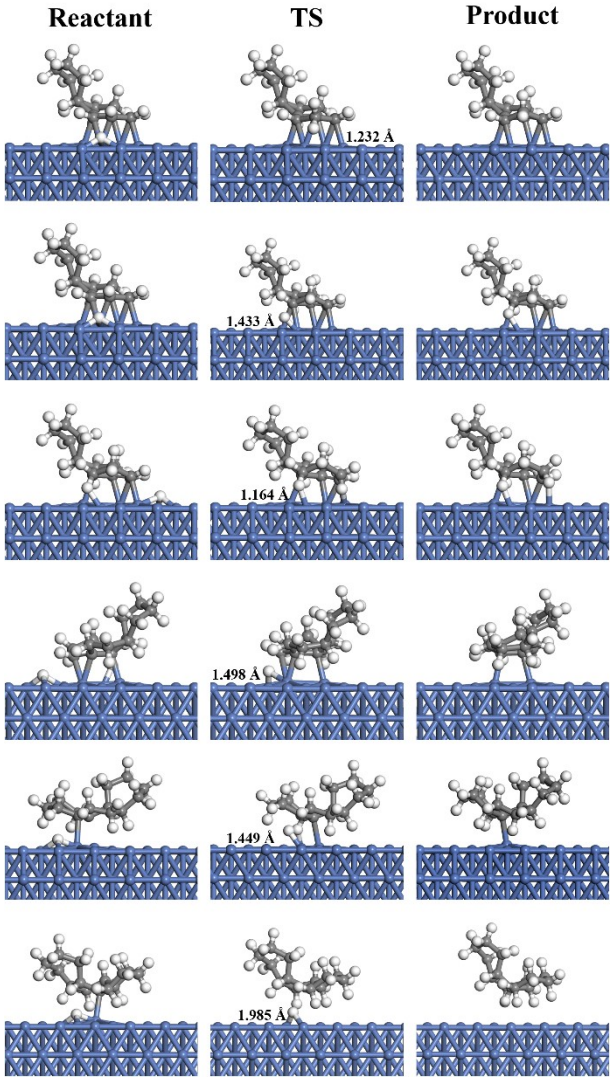

Figure S9. Optimized reactant, transition state, and product structures for the last- aromatic ring hydrogenation reaction of PHE on the Ni(111) surface. The first row: 9C+1H; the second row: 5C+2H; the third row: 6C+3H; the fourth row: 4C+4H; the fifth row: 2C+5H; the sixth row: 7C+6H.

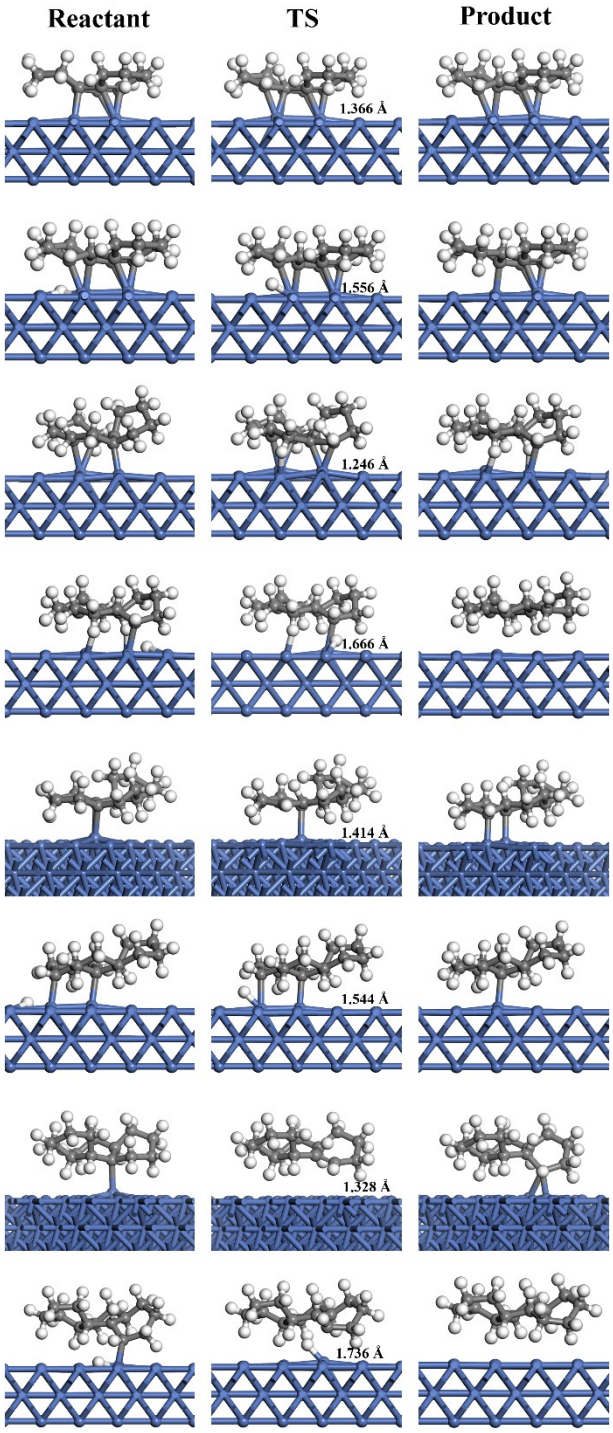

Figure S10. Optimized of reactants, transition states, and products structures for the formation of trans configurations of 8C, 13C, 2C, and 7C of PHE on the Ni(100) surface. The first row: 8C Htrans; the second row: 9C+H; the third row: 13C Htrans; the fourth row: 12C+H; the fifth row: 2C Htrans; the sixth row: 3C+H; the seventh row: 7C Htrans; the eighth row: 6C+H.

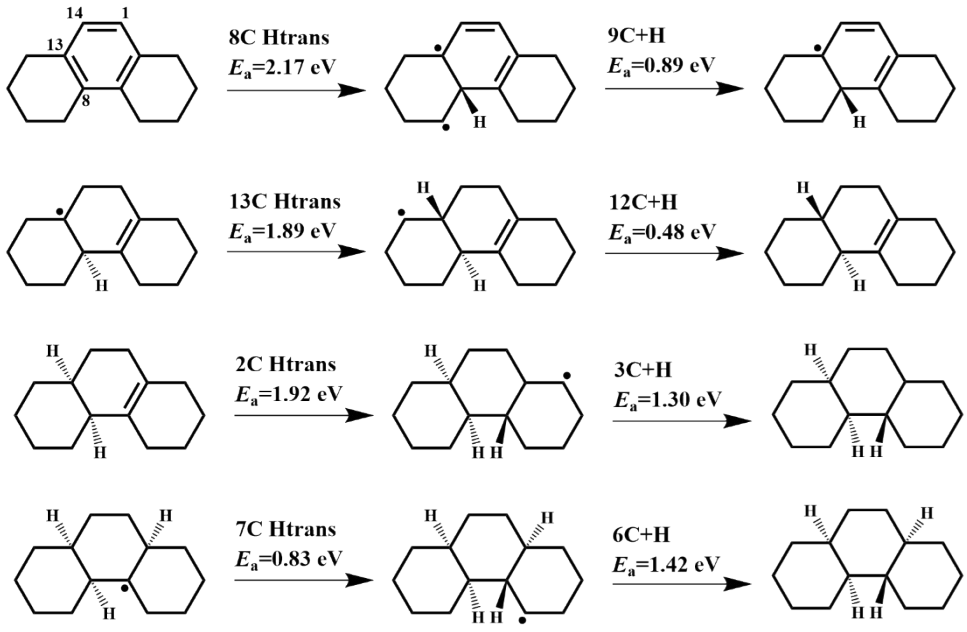

Figure S11. Reaction networks for the formation of trans configurations of 8C, 13C, 2C, and 7C of PHE on the Ni(100) surface.

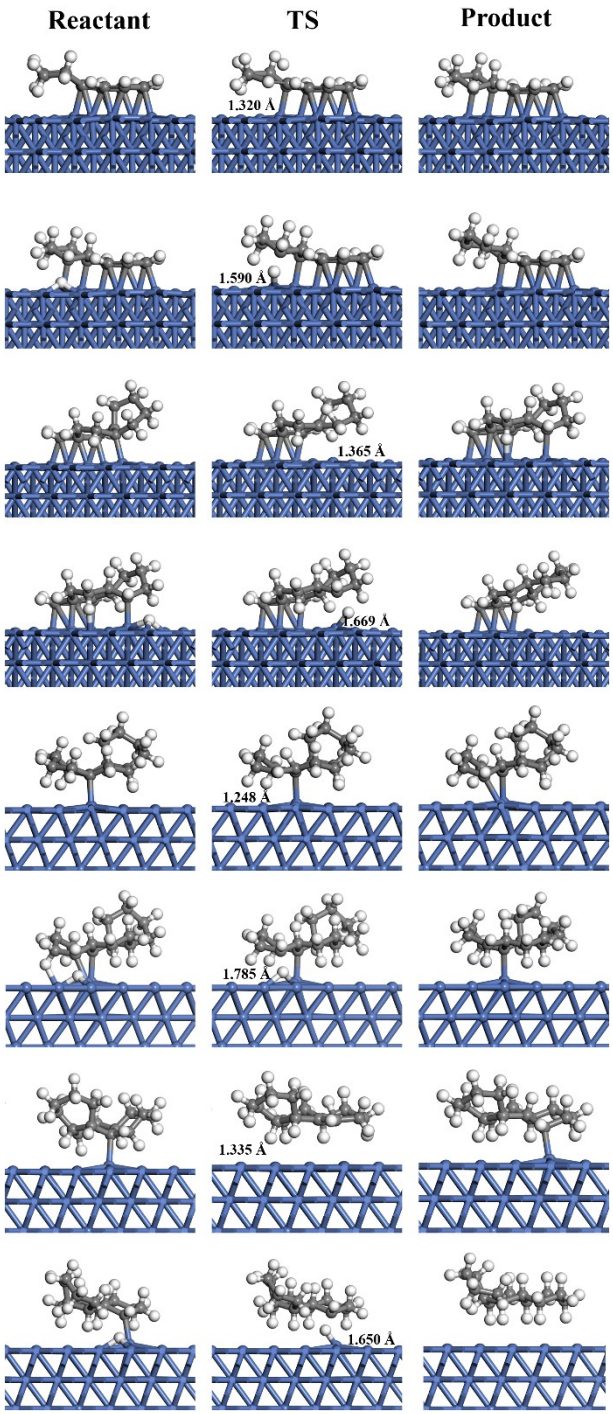

Figure S12. Optimized of reactants, transition states, and products structures for the formation of trans configurations of 8C, 13C, 2C, and 7C of PHE on the Ni(111) surface. The first row: 8C Htrans; the second row: 9C+H; the third row: 13C Htrans; the fourth row: 12C+H; the fifth row: 2C Htrans; the sixth row: 3C+H; the seventh row: 7C Htrans; the eighth row: 6C+H.

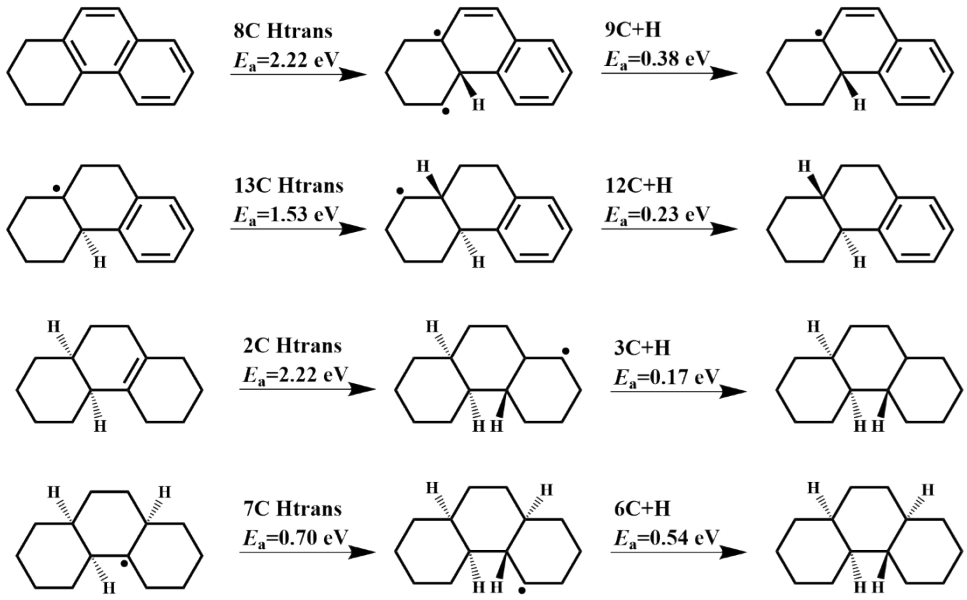

Figure S13. Reaction networks for the formation of trans configurations of 8C, 13C, 2C, and 7C of PHE on the Ni(111) surface.

3. Microkinetic modeling

A microkinetic modeling was established to investigate the changes in reaction rates and product selectivity of PHE hydrogenation at different temperatures. The forward reaction rates were used to approximately estimate the entire process. The elementary reactions are as follows:

R1 $PHE + * \xrightarrow{k_{PHE}} PHE*$

R2 $H_2 + 2* \xrightarrow{k_H} 2H*$

R3 $PHE* + H* \xrightarrow{k_1} PHE1H* + *$

R4 $PHE1H* + H* \xrightarrow{k_2} PHE2H* + *$

R5 $PHE2H* + H* \xrightarrow{k_3} PHE3H* + *$

R6 $PHE3H* + H* \xrightarrow{k_4} PHE4H* + *$

R7 $PHE4H* + H* \xrightarrow{k_5} PHE5H* + *$

R8 $PHE5H* + H* \xrightarrow{k_6} PHE6H* + *$

R9 $PHE6H* + H* \xrightarrow{k_7} PHE7H* + *$

R10 $PHE7H* + H* \xrightarrow{k_8} PHE8H* + *$

R11 $PHE8H* + H* \xrightarrow{k_9} PHE9H* + *$

R12 $PHE9H* + H* \xrightarrow{k_{10}} PHE10H* + *$

R13 $PHE10H* + H* \xrightarrow{k_{11}} PHE11H* + *$

R14 $PHE11H* + H* \xrightarrow{k_{12}} PHE12H*$

R15 $PHE12H* + H* \xrightarrow{k_{13}} PHE13H*$

R16 $PHE13H* + H* \xrightarrow{k_{14}} cis\text{-}syn\text{-}cis\text{-}PHP* + *$

R17 $PHE13H* \xrightarrow{k_{15}} PHE13H_{trans}*$

R18 $\mathrm{PHE13H_{trans}} * + \mathrm{H} * \xrightarrow{k_{16}} \mathrm{trans\text{-}anti\text{-}cis\text{-}PHP} * + *$

R19 $\mathrm{cis\text{-}syn\text{-}cis\text{-}PHP} * \xrightarrow{k_{\mathrm{des1}}} \mathrm{cis\text{-}syn\text{-}cis\text{-}PHP} + *$

R20 $\mathrm{trans\text{-}anti\text{-}cis\text{-}PHP} * \xrightarrow{k_{\mathrm{des2}}} \mathrm{trans\text{-}anti\text{-}cis\text{-}PHP} + *$

Among them, R1 and R2 represent the adsorption processes of PHE and hydrogen, and R3−R18 are the elementary reactions for forming cis-syn-cis PHP and trans-anti-cis PHP. The species coverages (θ) of reactants and products can be calculated by the following formulas:

$$\theta_{\mathrm{PHE}} = c_{\mathrm{PHE}} k_{\mathrm{PHE}} \theta *$$

$$\theta_{\mathrm{H}} = c_{\mathrm{H_2}}^{\frac{1}{2}} k_{\mathrm{H}} \theta *$$

The steady-state approximation was applied to R3–R20:

$$\frac{\mathrm{d}\theta_{\mathrm{PHE1H}}}{\mathrm{d}t} = k_1 \theta_{\mathrm{PHE}} \theta_{\mathrm{H}} - k_2 \theta_{\mathrm{PHE1H}} \theta_{\mathrm{H}} = 0$$

$$\frac{\mathrm{d}\theta_{\mathrm{PHE2H}}}{\mathrm{d}t} = k_2 \theta_{\mathrm{PHE1H}} \theta_{\mathrm{H}} - k_3 \theta_{\mathrm{PHE2H}} \theta_{\mathrm{H}} = 0$$

$$\frac{\mathrm{d}\theta_{\mathrm{PHE3H}}}{\mathrm{d}t} = k_3 \theta_{\mathrm{PHE2H}} \theta_{\mathrm{H}} - k_4 \theta_{\mathrm{PHE3H}} \theta_{\mathrm{H}} = 0$$

$$\frac{\mathrm{d}\theta_{\mathrm{PHE4H}}}{\mathrm{d}t} = k_4 \theta_{\mathrm{PHE3H}} \theta_{\mathrm{H}} - k_5 \theta_{\mathrm{PHE4H}} \theta_{\mathrm{H}} = 0$$

$$\frac{\mathrm{d}\theta_{\mathrm{PHE5H}}}{\mathrm{d}t} = k_5 \theta_{\mathrm{PHE4H}} \theta_{\mathrm{H}} - k_6 \theta_{\mathrm{PHE5H}} \theta_{\mathrm{H}} = 0$$

$$\frac{\mathrm{d}\theta_{\mathrm{PHE6H}}}{\mathrm{d}t} = k_6 \theta_{\mathrm{PHE5H}} \theta_{\mathrm{H}} - k_7 \theta_{\mathrm{PHE6H}} \theta_{\mathrm{H}} = 0$$

$$\frac{\mathrm{d}\theta_{\mathrm{PHE7H}}}{\mathrm{d}t} = k_7 \theta_{\mathrm{PHE6H}} \theta_{\mathrm{H}} - k_8 \theta_{\mathrm{PHE7H}} \theta_{\mathrm{H}} = 0$$

$$\frac{\mathrm{d}\theta_{\mathrm{PHE8H}}}{\mathrm{d}t} = k_8 \theta_{\mathrm{PHE7H}} \theta_{\mathrm{H}} - k_9 \theta_{\mathrm{PHE8H}} \theta_{\mathrm{H}} = 0$$

$$\frac{\mathrm{d}\theta_{\mathrm{PHE9H}}}{\mathrm{d}t} = k_9 \theta_{\mathrm{PHE8H}} \theta_{\mathrm{H}} - k_{10} \theta_{\mathrm{PHE9H}} \theta_{\mathrm{H}} = 0$$

$$\frac{\mathrm{d}\theta_{\mathrm{PHE10H}}}{\mathrm{d}t} = k_{10} \theta_{\mathrm{PHE9H}} \theta_{\mathrm{H}} - k_{11} \theta_{\mathrm{PHE10H}} \theta_{\mathrm{H}} = 0$$

$$\frac{\mathrm{d}\theta_{\mathrm{PHE11H}}}{\mathrm{d}t} = k_{11} \theta_{\mathrm{PHE10H}} \theta_{\mathrm{H}} - k_{12} \theta_{\mathrm{PHE11H}} \theta_{\mathrm{H}} = 0$$

$$\frac{\mathrm{d}\theta_{\mathrm{PHE12H}}}{\mathrm{d}t} = k_{12}\theta_{\mathrm{PHE11H}}\theta_{\mathrm{H}} - k_{13}\theta_{\mathrm{PHE12H}}\theta_{\mathrm{H}} = 0$$

$$\frac{\mathrm{d}\theta_{\mathrm{PHE13H}}}{\mathrm{d}t} = k_{13}\theta_{\mathrm{PHE12H}}\theta_{\mathrm{H}} - k_{14}\theta_{\mathrm{PHE13H}}\theta_{\mathrm{H}} - k_{15}\theta_{\mathrm{PHE13H}} = 0$$

$$\frac{\mathrm{d}\theta_{\mathrm{cis\text{-}syn\text{-}cis\text{-}PHP}}}{\mathrm{d}t} = k_{14}\theta_{\mathrm{PHE13H}}\theta_{\mathrm{H}} - k_{des1}\theta_{\mathrm{cis\text{-}syn\text{-}cis\text{-}PHP}} = 0$$

$$\frac{\mathrm{d}\theta_{\mathrm{PHE13H\text{-}trans}}}{\mathrm{d}t} = k_{15}\theta_{\mathrm{PHE13H}} - k_{16}\theta_{\mathrm{PHE13H\text{-}trans}}\theta_{\mathrm{H}} = 0$$

$$\frac{\mathrm{d}\theta_{\mathrm{trans\text{-}anti\text{-}cis\text{-}PHP}}}{\mathrm{d}t} = k_{16}\theta_{\mathrm{PHE13H\text{-}trans}}\theta_{\mathrm{H}} - k_{des2}\theta_{\mathrm{trans\text{-}anti\text{-}cis\text{-}PHP}} = 0$$

The relationship of all coverages is:

$$\theta^{*} + \sum_{j \neq *} \theta_{j} = 1$$

The calculation results of k and θ at different temperatures are shown in Table S11-23.

The reaction rates for the formation of cis-syn-cis-PHP and trans-anti-cis-PHP can be calculated using the following formula.

$$\gamma_{\mathrm{cis\text{-}syn\text{-}cis\text{-}PHP}} = k_{14}\theta_{\mathrm{H}}\theta_{\mathrm{cis\text{-}syn\text{-}cis\text{-}PHP}}$$

$$\gamma_{\mathrm{trans\text{-}anti\text{-}cis\text{-}PHP}} = k_{16}\theta_{\mathrm{H}}\theta_{\mathrm{trans\text{-}anti\text{-}cis\text{-}PHP}}$$

The selectivity of cis-syn-cis-PHP and trans-anti-cis-PHP were calculated using the following Equation.

$$S = \frac{\gamma_{\mathrm{cis\text{-}syn\text{-}cis\text{-}PHP/trans\text{-}anti\text{-}cis\text{-}PHP}}}{\gamma_{\mathrm{cis\text{-}syn\text{-}cis\text{-}PHP}} + \gamma_{\mathrm{trans\text{-}anti\text{-}cis\text{-}PHP}}}$$

Table S9. ΔG_a (kJ/mol) for PHE hydrogenation on the Ni(100) surface

T(K)	533.15	553.15	573.15	593.15	613.15	633.15	653.15	673.15	693.15	713.15	733.15	753.15	773.15
PHE1H	68.14	68.12	68.11	68.11	68.11	68.12	68.14	68.16	68.18	68.22	68.25	68.30	68.34
PHE2H	64.78	65.02	65.26	65.52	65.78	66.05	66.33	66.61	66.90	67.20	67.50	67.81	68.13
PHE3H	65.70	65.90	66.11	66.33	66.56	66.79	67.03	67.28	67.53	67.79	68.06	68.33	68.61
PHE4H	36.52	36.67	36.83	36.99	37.17	37.34	37.53	37.72	37.92	38.12	38.33	38.54	38.76
PHE5H	82.95	83.25	83.57	83.89	84.22	84.56	84.90	85.26	85.61	85.98	86.35	86.72	87.10
PHE6H	67.95	68.12	68.29	68.47	68.66	68.86	69.06	69.27	69.49	69.72	69.95	70.18	70.42
PHE7H	72.86	73.48	74.10	74.74	75.39	76.04	76.71	77.39	78.08	78.77	79.48	80.19	80.91
PHE8H	62.78	62.53	62.29	62.04	61.80	61.56	61.32	61.08	60.85	60.61	60.38	60.15	59.92
PHE9H	92.12	91.52	90.91	90.30	89.68	89.06	88.43	87.80	87.17	86.53	85.89	85.25	84.60
PHE10H	68.70	68.80	68.91	69.02	69.15	69.28	69.42	69.56	69.71	69.87	70.03	70.20	70.38
PHE11H	24.77	24.85	24.93	25.03	25.13	25.24	25.36	25.49	25.63	25.78	25.93	26.09	26.26
PHE12H	125.61	126.25	126.91	127.60	128.31	129.04	129.79	130.57	131.36	132.18	133.01	133.86	134.73
PHE13H	54.50	54.70	54.91	55.13	55.34	55.56	55.79	56.02	56.26	56.50	56.74	56.99	57.24
cis-syn-cis PHP	26.63	26.31	26.00	25.69	25.38	25.07	24.77	24.46	24.16	23.86	23.56	23.26	22.96
PHE13H-trans	133.80	134.92	136.05	137.21	138.39	139.59	140.80	142.04	143.29	144.56	145.85	147.15	148.47
trans-anti-cis PHP	61.01	60.54	60.07	59.60	59.13	58.67	58.20	57.73	57.27	56.81	56.34	55.88	55.42
cis-syn-cis-PHP_{des}	-146.17	-146.14	-146.11	-146.08	-146.06	-146.03	-146.01	-146.00	-145.98	-145.97	-145.96	-145.95	-145.94
trans-anti-cis-PHP_{des}	-207.78	-209.06	-210.35	-211.67	-213.01	-214.36	-215.74	-217.13	-218.54	-219.97	-221.41	-222.88	-224.35

Table S10. ΔG_a (kJ/mol) for PHE hydrogenation on the Ni(111) surface

T(K)	533.15	553.15	573.15	593.15	613.15	633.15	653.15	673.15	693.15	713.15	733.15	753.15	773.15
PHE1H	70.70	70.91	71.12	71.34	71.56	71.79	72.02	72.26	72.51	72.76	73.01	73.27	73.53
PHE2H	18.50	18.62	18.74	18.86	18.99	19.12	19.26	19.40	19.54	19.69	19.84	20.00	20.15
PHE3H	81.65	82.05	82.46	82.88	83.31	83.76	84.21	84.67	85.14	85.62	86.11	86.61	87.12
PHE4H	33.82	33.89	33.96	34.03	34.11	34.20	34.29	34.38	34.48	34.58	34.69	34.80	34.91
PHE5H	64.08	64.43	64.78	65.14	65.51	65.89	66.28	66.67	67.07	67.48	67.90	68.32	68.75
PHE6H	15.45	15.60	15.76	15.91	16.07	16.23	16.39	16.56	16.72	16.89	17.06	17.23	17.41
PHE7H	15.59	14.75	13.90	13.03	12.17	11.29	10.41	9.52	8.63	7.73	6.83	5.92	5.00
PHE8H	56.98	56.43	55.88	55.33	54.77	54.21	53.65	53.09	52.53	51.97	51.40	50.84	50.27
PHE9H	79.53	80.18	80.83	81.50	82.18	82.87	83.57	84.28	85.00	85.73	86.47	87.22	87.98
PHE10H	23.08	23.16	23.25	23.34	23.44	23.53	23.64	23.74	23.85	23.97	24.08	24.20	24.33
PHE11H	16.41	16.39	16.38	16.38	16.38	16.38	16.39	16.40	16.42	16.44	16.46	16.49	16.52
PHE12H	60.54	61.01	61.48	61.96	62.45	62.96	63.47	63.99	64.52	65.05	65.60	66.15	66.72
PHE13H	67.38	68.18	69.00	69.83	70.67	71.53	72.41	73.29	74.19	75.10	76.03	76.97	77.92
cis-syn-cis PHP	-1.40	-1.76	-2.11	-2.46	-2.82	-3.18	-3.54	-3.90	-4.26	-4.62	-4.99	-5.35	-5.72
PHE13H-trans	85.86	85.78	85.70	85.63	85.56	85.50	85.44	85.38	85.33	85.29	85.24	85.20	85.16
trans-anti-cis PHP	33.90	33.33	32.76	32.18	31.61	31.03	30.46	29.88	29.30	28.72	28.14	27.56	26.99
cis-syn-cis-PHP_{des}	-161.85	-162.59	-163.34	-164.10	-164.87	-165.66	-166.46	-167.26	-168.08	-168.92	-169.76	-170.61	-171.48
trans-anti-cis-PHP_{des}	-175.89	-175.73	-175.57	-175.42	-175.26	-175.11	-174.97	-174.82	-174.68	-174.54	-174.40	-174.26	-174.13

Table S11. Reaction rate constants and coverage for elementary hydrogenation steps of PHE on Ni(100) and Ni(111) surfaces at 533 K.

Reaction	Rate constant (M^{-1} s^{-1})		Species	Coverage	
	Ni(100)	Ni(111)		Ni(100)	Ni(111)
R1	1.04E+06	4.51E+05	PHE	2.94E-09	2.94E−09
R2	4.96E+10	2.15E+10	H	1.00E+00	1.00E+00
R3	2.43E+06	1.35E+06	PHE1H	1.15E-09	1.93E-14
R4	6.22E+06	2.06E+11	PHE2H	1.39E-09	2.70E-08
R5	5.16E+06	1.47E+05	PHE3H	2.24E-12	6.56E-13
R6	3.20E+09	6.06E+09	PHE4H	6.87E-08	6.02E-10
R7	1.04E+05	6.61E+06	PHE5H	2.45E-09	1.13E-14
R8	2.92E+06	3.53E+11	PHE6H	8.83E-09	1.10E-14
R9	8.11E+05	3.62E+11	PHE7H	7.76E-10	1.05E-10
R10	9.23E+06	3.79E+07	PHE8H	5.42E-07	2.16E-08
R11	1.32E+04	1.84E+05	PHE9H	3.20E-09	5.50E-14
R12	2.24E+06	7.23E+10	PHE10H	1.71E-13	1.17E-14
R13	4.19E+10	3.39E+11	PHE11H	1.07E-03	2.63E-10
R14	6.67E+00	1.51E+07	PHE12H	1.13E-10	1.12E-09
R15	6.32E+07	3.54E+06	PHE13H	2.56E-13	2.47E-16
R16	2.80E+10	1.61E+13	cis-syn-cis PHP	2.36E-09	1.04E-07
R17	1.15E+00(s^{-1})	5.29E+04(s^{-1})	PHE13H-trans	1.99E-20	1.88E-21
R18	1.47E+07	6.92E+09	trans-anti-cis PHP	1.05E-13	8.09E-15
R19	3.04E+06	3.82E+04	*	1.90E-11	4.39E-11
R20	2.79E+00	1.61E+03			

Table S12. Reaction rate constants and coverage for elementary hydrogenation steps of PHE on Ni(100) and Ni(111) surfaces at 553 K.

Reaction	Rate constant (M^{-1} s^{-1})		Species	Coverage	
	Ni(100)	Ni(111)		Ni(100)	Ni(111)
R1	1.06E+06	4.59E+05	PHE	3.11E-09	3.11E-09
R2	4.87E+10	2.11E+10	H	1.00E+00	1.00E+00
R3	4.41E+06	2.38E+06	PHE1H	1.33E-09	3.10E-14
R4	1.03E+07	2.39E+11	PHE2H	1.59E-09	2.77E-08
R5	8.62E+06	2.68E+05	PHE3H	3.18E-12	9.15E-13
R6	4.30E+09	8.10E+09	PHE4H	6.98E-08	6.97E-10
R7	1.96E+05	1.06E+07	PHE5H	2.73E-09	1.85E-14
R8	5.02E+06	4.01E+11	PHE6H	1.03E-08	1.45E-14
R9	1.33E+06	5.10E+11	PHE7H	8.21E-10	1.07E-10
R10	1.67E+07	6.93E+07	PHE8H	4.19E-07	2.33E-08
R11	3.26E+04	3.18E+05	PHE9H	3.46E-09	8.43E-14
R12	3.95E+06	8.79E+10	PHE10H	2.61E-13	1.87E-14
R13	5.24E+10	3.98E+11	PHE11H	8.26E-04	3.22E-10
R14	1.66E+01	2.30E+07	PHE12H	1.42E-10	1.41E-09
R15	9.65E+07	5.26E+06	PHE13H	3.55E-13	4.17E-16
R16	3.85E+10	1.78E+13	cis-syn-cis PHP	1.22E-09	5.45E-08
R17	2.73E+00(s^{-1})	1.11E+05(s^{-1})	PHE13H-trans	3.54E-20	4.38E-21
R18	2.74E+07	1.05E+10	trans-anti-cis PHP	7.54E-14	5.91E-15
R19	1.13E+07	1.36E+05	*	1.97E-11	4.56E-11
R20	1.29E+01	7.82E+03			

Table S13. Reaction rate constants and coverage for elementary hydrogenation steps of PHE on Ni(100) and Ni(111) surfaces at 573 K.

Reaction	Rate constant (M^{-1} s^{-1})		Species	Coverage	
	Ni(100)	Ni(111)		Ni(100)	Ni(111)
R1	1.08E+06	4.68E+05	PHE	3.28E-09	3.28E-09
R2	4.78E+10	2.07E+10	H	1.00E+00	1.00E+00
R3	7.65E+06	4.04E+06	PHE1H	1.54E-09	4.81E-14
R4	1.63E+07	2.75E+11	PHE2H	1.80E-09	2.84E-08
R5	1.39E+07	4.67E+05	PHE3H	4.43E-12	1.25E-12
R6	5.67E+09	1.06E+10	PHE4H	7.10E-08	7.99E-10
R7	3.53E+05	1.66E+07	PHE5H	3.01E-09	2.93E-14
R8	8.32E+06	4.51E+11	PHE6H	1.19E-08	1.88E-14
R9	2.12E+06	7.02E+11	PHE7H	8.65E-10	1.09E-10
R10	2.90E+07	1.22E+08	PHE8H	3.30E-07	2.52E-08
R11	7.59E+04	5.26E+05	PHE9H	3.73E-09	1.25E-13
R12	6.72E+06	1.06E+11	PHE10H	3.90E-13	2.87E-14
R13	6.43E+10	4.62E+11	PHE11H	6.51E-04	3.89E-10
R14	3.85E+01	3.40E+07	PHE12H	1.75E-10	1.74E-09
R15	1.43E+08	7.60E+06	PHE13H	4.83E-13	6.78E-16
R16	5.20E+10	1.95E+13	cis-syn-cis PHP	6.56E-10	2.98E-08
R17	6.11E+00(s^{-1})	2.21E+05(s^{-1})	PHE13H-trans	6.01E-20	9.61E-21
R18	4.90E+07	1.56E+10	trans-anti-cis PHP	5.53E-14	4.40E-15
R19	3.82E+07	4.44E+05	*	2.04E-11	4.72E-11
R20	5.33E+01	3.41E+04			

Table S14. Reaction rate constants and coverage for elementary hydrogenation steps of PHE on Ni(100) and Ni(111) surfaces at 593 K.

Reaction	Rate constant (M^{-1} s^{-1})		Species	Coverage	
	Ni(100)	Ni(111)		Ni(100)	Ni(111)
R1	1.10E+06	4.76E+05	PHE	3.46E-09	3.46E-09
R2	4.70E+10	2.03E+10	H	1.00E+00	1.00E+00
R3	1.28E+07	6.61E+06	PHE1H	1.76E-09	7.28E-14
R4	2.52E+07	3.14E+11	PHE2H	2.04E-09	2.92E-08
R5	2.17E+07	7.83E+05	PHE3H	6.05E-12	1.67E-12
R6	7.32E+09	1.37E+10	PHE4H	7.25E-08	9.13E-10
R7	6.11E+05	2.50E+07	PHE5H	3.32E-09	4.52E-14
R8	1.33E+07	5.05E+11	PHE6H	1.36E-08	2.40E-14
R9	3.25E+06	9.50E+11	PHE7H	9.13E-10	1.11E-10
R10	4.85E+07	2.07E+08	PHE8H	2.65E-07	2.72E-08
R11	1.67E+05	8.41E+05	PHE9H	4.02E-09	1.82E-13
R12	1.10E+07	1.25E+11	PHE10H	5.69E-13	4.30E-14
R13	7.79E+10	5.31E+11	PHE11H	5.26E-04	4.67E-10
R14	8.42E+01	4.89E+07	PHE12H	2.14E-10	2.14E-09
R15	2.07E+08	1.07E+07	PHE13H	6.44E-13	1.07E-15
R16	6.87E+10	2.13E+13	cis-syn-cis PHP	3.71E-10	1.71E-08
R17	1.29E+01(s^{-1})	4.22E+05(s^{-1})	PHE13H-trans	9.83E-20	1.99E-20
R18	8.43E+07	2.26E+10	trans-anti-cis PHP	4.14E-14	3.34E-15
R19	1.20E+08	1.34E+06	*	2.12E-11	4.89E-11
R20	2.00E+02	1.35E+05			

Table S15. Reaction rate constants and coverage for elementary hydrogenation steps of PHE on Ni(100) and Ni(111) surfaces at 613 K.

Reaction	Rate constant (M^{-1} s^{-1})		Species	Coverage	
	Ni(100)	Ni(111)		Ni(100)	Ni(111)
R1	1.12E+06	4.84E+05	PHE	3.63E-09	3.63E-09
R2	4.62E+10	2.00E+10	H	1.00E+00	1.00E+00
R3	2.07E+07	1.05E+07	PHE1H	1.99E-09	1.07E-13
R4	3.77E+07	3.55E+11	PHE2H	2.29E-09	2.99E-08
R5	3.29E+07	1.27E+06	PHE3H	8.08E-12	2.19E-12
R6	9.30E+09	1.73E+10	PHE4H	7.38E-08	1.03E-09
R7	1.02E+06	3.68E+07	PHE5H	3.63E-09	6.76E-14
R8	2.07E+07	5.61E+11	PHE6H	1.55E-08	3.01E-14
R9	4.85E+06	1.26E+12	PHE7H	9.56E-10	1.12E-10
R10	7.86E+07	3.39E+08	PHE8H	2.14E-07	2.92E-08
R11	3.51E+05	1.30E+06	PHE9H	4.30E-09	2.58E-13
R12	1.75E+07	1.47E+11	PHE10H	8.08E-13	6.27E-14
R13	9.30E+10	6.06E+11	PHE11H	4.31E-04	5.53E-10
R14	1.74E+02	6.86E+07	PHE12H	2.57E-10	2.58E-09
R15	2.92E+08	1.47E+07	PHE13H	8.41E-13	1.64E-15
R16	8.94E+10	2.32E+13	cis-syn-cis PHP	2.16E-10	1.01E-08
R17	2.59E+01(s^{-1})	7.70E+05(s^{-1})	PHE13H-trans	1.55E-19	3.95E-20
R18	1.40E+08	3.19E+10	trans-anti-cis PHP	3.15E-14	2.57E-15
R19	3.49E+08	3.77E+06	*	2.19E-11	5.05E-11
R20	6.91E+02	4.91E+05			

Table S16. Reaction rate constants and coverage for elementary hydrogenation steps of PHE on Ni(100) and Ni(111) surfaces at 633 K.

Reaction	Rate constant (M^{-1} s^{-1})		Species	Coverage	
	Ni(100)	Ni(111)		Ni(100)	Ni(111)
R1	1.14E+06	4.91E+05	PHE	3.80E-09	3.80E-09
R2	4.55E+10	1.97E+10	H	1.00E+00	1.00E+00
R3	3.25E+07	1.61E+07	PHE1H	2.25E-09	1.53E-13
R4	5.51E+07	3.99E+11	PHE2H	2.55E-09	3.07E-08
R5	4.85E+07	2.00E+06	PHE3H	1.06E-11	2.83E-12
R6	1.16E+10	2.16E+10	PHE4H	7.51E-08	1.16E-09
R7	1.65E+06	5.27E+07	PHE5H	3.96E-09	9.87E-14
R8	3.13E+07	6.20E+11	PHE6H	1.75E-08	3.70E-14
R9	7.05E+06	1.65E+12	PHE7H	9.99E-10	1.13E-10
R10	1.24E+08	5.40E+08	PHE8H	1.76E-07	3.12E-08
R11	7.03E+05	1.96E+06	PHE9H	4.60E-09	3.58E-13
R12	2.69E+07	1.71E+11	PHE10H	1.13E-12	8.93E-14
R13	1.10E+11	6.85E+11	PHE11H	3.60E-04	6.50E-10
R14	3.44E+02	9.42E+07	PHE12H	3.07E-10	3.10E-09
R15	4.03E+08	1.98E+07	PHE13H	1.08E-12	2.44E-15
R16	1.14E+11	2.51E+13	cis-syn-cis PHP	1.30E-10	6.16E-09
R17	4.95E+01(s^{-1})	1.36E+06(s^{-1})	PHE13H-trans	2.37E-19	7.47E-20
R18	2.26E+08	4.42E+10	trans-anti-cis PHP	2.43E-14	2.01E-15
R19	9.54E+08	9.92E+06	*	2.25E-11	5.21E-11
R20	2.20E+03	1.65E+06			

Table S17. Reaction rate constants and coverage for elementary hydrogenation steps of PHE on Ni(100) and Ni(111) surfaces at 653 K.

Reaction	Rate constant (M^{-1} s^{-1})		Species	Coverage	
	Ni(100)	Ni(111)		Ni(100)	Ni(111)
R1	1.15E+06	4.99E+05	PHE	3.99E-09	3.99E-09
R2	4.48E+10	1.94E+10	H	1.00E+00	1.00E+00
R3	4.96E+07	2.41E+07	PHE1H	2.52E-09	2.16E-13
R4	7.86E+07	4.45E+11	PHE2H	2.83E-09	3.15E-08
R5	7.00E+07	3.05E+06	PHE3H	1.38E-11	3.61E-12
R6	1.44E+10	2.67E+10	PHE4H	7.67E-08	1.30E-09
R7	2.58E+06	7.40E+07	PHE5H	4.31E-09	1.41E-13
R8	4.60E+07	6.81E+11	PHE6H	1.98E-08	4.51E-14
R9	1.00E+07	2.13E+12	PHE7H	1.05E-09	1.15E-10
R10	1.90E+08	8.38E+08	PHE8H	1.46E-07	3.35E-08
R11	1.35E+06	2.87E+06	PHE9H	4.91E-09	4.88E-13
R12	4.04E+07	1.97E+11	PHE10H	1.54E-12	1.25E-13
R13	1.28E+11	7.70E+11	PHE11H	3.05E-04	7.59E-10
R14	6.49E+02	1.27E+08	PHE12H	3.63E-10	3.69E-09
R15	5.46E+08	2.61E+07	PHE13H	1.37E-12	3.55E-15
R16	1.44E+11	2.71E+13	cis-syn-cis PHP	8.08E-11	3.90E-09
R17	9.09E+01(s^{-1})	2.31E+06(s^{-1})	PHE13H-trans	3.53E-19	1.36E-19
R18	3.54E+08	6.01E+10	trans-anti-cis PHP	1.91E-14	1.59E-15
R19	2.46E+09	2.47E+07	*	2.33E-11	5.38E-11
R20	6.53E+03	5.14E+06			

Table S18. Reaction rate constants and coverage for elementary hydrogenation steps of PHE on Ni(100) and Ni(111) surfaces at 673 K.

Reaction	Rate constant (M^{-1} s^{-1})		Species	Coverage	
	Ni(100)	Ni(111)		Ni(100)	Ni(111)
R1	1.17E+06	5.07E+05	PHE	4.18E-09	4.17E-09
R2	4.41E+10	1.91E+10	H	1.00E+00	1.00E+00
R3	7.39E+07	3.53E+07	PHE1H	2.81E-09	2.98E-13
R4	1.10E+08	4.94E+11	PHE2H	3.13E-09	3.24E-08
R5	9.87E+07	4.54E+06	PHE3H	1.76E-11	4.53E-12
R6	1.75E+10	3.24E+10	PHE4H	7.82E-08	1.45E-09
R7	3.94E+06	1.02E+08	PHE5H	4.66E-09	1.98E-13
R8	6.62E+07	7.45E+11	PHE6H	2.22E-08	5.41E-14
R9	1.39E+07	2.72E+12	PHE7H	1.09E-09	1.16E-10
R10	2.83E+08	1.27E+09	PHE8H	1.23E-07	3.57E-08
R11	2.51E+06	4.12E+06	PHE9H	5.22E-09	6.53E-13
R12	5.91E+07	2.25E+11	PHE10H	2.08E-12	1.71E-13
R13	1.48E+11	8.59E+11	PHE11H	2.62E-04	8.78E-10
R14	1.18E+03	1.68E+08	PHE12H	4.24E-10	4.36E-09
R15	7.27E+08	3.38E+07	PHE13H	1.72E-12	5.04E-15
R16	1.80E+11	2.92E+13	cis-syn-cis PHP	5.15E-11	2.53E-09
R17	1.61E+02(s^{-1})	3.80E+06(s^{-1})	PHE13H-trans	5.10E-19	2.39E-19
R18	5.40E+08	8.04E+10	trans-anti-cis PHP	1.52E-14	1.27E-15
R19	6.00E+09	5.81E+07	*	2.40E-11	5.54E-11
R20	1.81E+04	1.50E+07			

Table S19. Reaction rate constants and coverage for elementary hydrogenation steps of PHE on Ni(100) and Ni(111) surfaces at 693 K.

Reaction	Rate constant (M^{-1} s^{-1})		Species	Coverage	
	Ni(100)	Ni(111)		Ni(100)	Ni(111)
R1	1.19E+06	5.14E+05	PHE	4.36E-09	4.36E-09
R2	4.35E+10	1.88E+10	H	9.99E-01	1.00E+00
R3	1.07E+08	5.05E+07	PHE1H	3.11E-09	4.04E-13
R4	1.50E+08	5.45E+11	PHE2H	3.43E-09	3.34E-08
R5	1.36E+08	6.60E+06	PHE3H	2.22E-11	5.64E-12
R6	2.11E+10	3.91E+10	PHE4H	7.96E-08	1.61E-09
R7	5.88E+06	1.37E+08	PHE5H	5.02E-09	2.72E-13
R8	9.33E+07	8.10E+11	PHE6H	2.47E-08	6.44E-14
R9	1.89E+07	3.42E+12	PHE7H	1.13E-09	1.17E-10
R10	4.14E+08	1.87E+09	PHE8H	1.04E-07	3.82E-08
R11	4.50E+06	5.77E+06	PHE9H	5.54E-09	8.61E-13
R12	8.46E+07	2.56E+11	PHE10H	2.75E-12	2.31E-13
R13	1.70E+11	9.53E+11	PHE11H	2.28E-04	1.01E-09
R14	2.06E+03	2.18E+08	PHE12H	4.92E-10	5.12E-09
R15	9.52E+08	4.30E+07	PHE13H	2.12E-12	7.04E-15
R16	2.21E+11	3.13E+13	cis-syn-cis PHP	3.36E-11	1.69E-09
R17	2.74E+02(s^{-1})	6.09E+06(s^{-1})	PHE13H-trans	7.22E-19	4.05E-19
R18	8.05E+08	1.06E+11	trans-anti-cis PHP	1.22E-14	1.03E-15
R19	1.39E+10	1.30E+08	*	2.47E-11	5.71E-11
R20	4.75E+04	4.15E+07			

Table S20. Reaction rate constants and coverage for elementary hydrogenation steps of PHE on Ni(100) and Ni(111) surfaces at 713 K.

Reaction	Rate constant (M^{-1} s^{-1})		Species	Coverage	
	Ni(100)	Ni(111)		Ni(100)	Ni(111)
R1	1.21E+06	5.22E+05	PHE	2.54E-11	5.88E-11
R2	4.29E+10	1.86E+10	H	4.55E-09	4.56E-09
R3	1.53E+08	7.08E+07	PHE1H	1.00E+00	1.00E+00
R4	2.02E+08	5.97E+11	PHE2H	3.44E-09	5.40E-13
R5	1.85E+08	9.39E+06	PHE3H	3.76E-09	3.44E-08
R6	2.52E+10	4.65E+10	PHE4H	2.76E-11	6.93E-12
R7	8.57E+06	1.82E+08	PHE5H	8.13E-08	1.78E-09
R8	1.29E+08	8.78E+11	PHE6H	5.40E-09	3.67E-13
R9	2.53E+07	4.26E+12	PHE7H	2.75E-08	7.58E-14
R10	5.93E+08	2.72E+09	PHE8H	1.17E-09	1.19E-10
R11	7.82E+06	7.93E+06	PHE9H	8.90E-08	4.07E-08
R12	1.19E+08	2.88E+11	PHE10H	5.87E-09	1.12E-12
R13	1.93E+11	1.05E+12	PHE11H	3.60E-12	3.07E-13
R14	3.47E+03	2.79E+08	PHE12H	2.01E-04	1.16E-09
R15	1.23E+09	5.40E+07	PHE13H	5.67E-10	5.97E-09
R16	2.69E+11	3.34E+13	cis-syn-cis PHP	2.59E-12	9.65E-15
R17	4.53E+02(s^{-1})	9.50E+06(s^{-1})	PHE13H-trans	2.25E-11	1.16E-09
R18	1.17E+09	1.37E+11	trans-anti-cis PHP	9.98E-19	6.67E-19
R19	3.10E+10	2.79E+08	*	9.97E-15	8.46E-16
R20	1.18E+05	1.08E+08			

Table S 21. Reaction rate constants and coverage for elementary hydrogenation steps of PHE on Ni(100) and Ni(111) surfaces at 733 K.

Reaction	Rate constant (M^{-1} s^{-1})		Species	Coverage	
	Ni(100)	Ni(111)		Ni(100)	Ni(111)
R1	1.22E+06	5.29E+05	PHE	4.74E-09	4.74E-09
R2	4.23E+10	1.83E+10	H	1.00E+00	1.00E+00
R3	2.14E+08	9.75E+07	PHE1H	3.79E-09	7.09E-13
R4	2.68E+08	6.52E+11	PHE2H	4.10E-09	3.53E-08
R5	2.47E+08	1.31E+07	PHE3H	3.41E-11	8.42E-12
R6	2.98E+10	5.49E+10	PHE4H	8.29E-08	1.95E-09
R7	1.22E+07	2.37E+08	PHE5H	5.80E-09	4.88E-13
R8	1.75E+08	9.48E+11	PHE6H	3.04E-08	8.81E-14
R9	3.33E+07	5.25E+12	PHE7H	1.22E-09	1.20E-10
R10	8.33E+08	3.86E+09	PHE8H	7.68E-08	4.32E-08
R11	1.32E+07	1.07E+07	PHE9H	6.21E-09	1.43E-12
R12	1.63E+08	3.23E+11	PHE10H	4.64E-12	4.01E-13
R13	2.18E+11	1.15E+12	PHE11H	1.78E-04	1.31E-09
R14	5.68E+03	3.52E+08	PHE12H	6.48E-10	6.91E-09
R15	1.56E+09	6.69E+07	PHE13H	3.13E-12	1.30E-14
R16	3.24E+11	3.57E+13	cis-syn-cis PHP	1.54E-11	8.04E-10
R17	7.27E+02(s^{-1})	1.45E+07(s^{-1})	PHE13H-trans	1.35E-18	1.07E-18
R18	1.68E+09	1.76E+11	trans-anti-cis PHP	8.20E-15	6.99E-16
R19	6.60E+10	5.75E+08	*	2.61E-11	6.04E-11
R20	2.78E+05	2.69E+08			

Table S22. Reaction rate constants and coverage for elementary hydrogenation steps of PHE on Ni(100) and Ni(111) surfaces at 753 K.

Reaction	Rate constant (M^{-1} s^{-1})		Species	Coverage	
	Ni(100)	Ni(111)		Ni(100)	Ni(111)
R1	1.24E+06	5.36E+05	PHE	4.95E-09	4.94E-09
R2	4.17E+10	1.81E+10	H	1.00E+00	1.00E+00
R3	2.93E+08	1.32E+08	PHE1H	4.16E-09	9.19E-13
R4	3.49E+08	7.09E+11	PHE2H	4.47E-09	3.63E-08
R5	3.25E+08	1.80E+07	PHE3H	4.17E-11	1.01E-11
R6	3.48E+10	6.43E+10	PHE4H	8.48E-08	2.14E-09
R7	1.71E+07	3.05E+08	PHE5H	6.22E-09	6.39E-13
R8	2.33E+08	1.02E+12	PHE6H	3.37E-08	1.02E-13
R9	4.31E+07	6.41E+12	PHE7H	1.26E-09	1.21E-10
R10	1.15E+09	5.39E+09	PHE8H	6.69E-08	4.59E-08
R11	2.17E+07	1.42E+07	PHE9H	6.57E-09	1.81E-12
R12	2.21E+08	3.60E+11	PHE10H	5.94E-12	5.17E-13
R13	2.45E+11	1.26E+12	PHE11H	1.61E-04	1.49E-09
R14	9.05E+03	4.38E+08	PHE12H	7.39E-10	7.96E-09
R15	1.96E+09	8.19E+07	PHE13H	3.76E-12	1.72E-14
R16	3.87E+11	3.79E+13	cis-syn-cis PHP	1.08E-11	5.72E-10
R17	1.14E+03(s^{-1})	2.16E+07(s^{-1})	PHE13H-trans	1.80E-18	1.67E-18
R18	2.36E+09	2.22E+11	trans-anti-cis PHP	6.84E-15	5.82E-16
R19	1.35E+11	1.14E+09	*	2.69E-11	6.20E-11
R20	6.25E+05	6.36E+08			

Table S23. Reaction rate constants and coverage for elementary hydrogenation steps of PHE on Ni(100) and Ni(111) surfaces at 773 K.

Reaction	Rate constant (M^{-1} s^{-1})		Species	Coverage	
	Ni(100)	Ni(111)		Ni(100)	Ni(111)
R1	1.25E+06	5.43E+05	PHE	5.15E-09	5.14E-09
R2	4.12E+10	1.78E+10	H	1.00E+00	1.00E+00
R3	3.96E+08	1.76E+08	PHE1H	4.54E-09	1.18E-12
R4	4.49E+08	7.68E+11	PHE2H	4.84E-09	3.74E-08
R5	4.21E+08	2.42E+07	PHE3H	5.04E-11	1.21E-11
R6	4.04E+10	7.46E+10	PHE4H	8.65E-08	2.34E-09
R7	2.36E+07	3.87E+08	PHE5H	6.64E-09	8.28E-13
R8	3.07E+08	1.09E+12	PHE6H	3.70E-08	1.17E-13
R9	5.51E+07	7.75E+12	PHE7H	1.30E-09	1.22E-10
R10	1.56E+09	7.40E+09	PHE8H	5.85E-08	4.87E-08
R11	3.49E+07	1.86E+07	PHE9H	6.92E-09	2.27E-12
R12	2.95E+08	3.99E+11	PHE10H	7.48E-12	6.60E-13
R13	2.72E+11	1.37E+12	PHE11H	1.45E-04	1.67E-09
R14	1.40E+04	5.40E+08	PHE12H	8.35E-10	9.13E-09
R15	2.44E+09	9.91E+07	PHE13H	4.46E-12	2.25E-14
R16	4.57E+11	4.03E+13	cis-syn-cis PHP	7.64E-12	4.15E-10
R17	1.73E+03(s^{-1})	3.15E+07(s^{-1})	PHE13H-trans	2.36E-18	2.55E-18
R18	3.26E+09	2.77E+11	trans-anti-cis PHP	5.73E-15	4.90E-16
R19	2.68E+11	2.18E+09	*	2.76E-11	6.37E-11
R20	1.35E+06	1.44E+09			

References

[1] Jiang Y, Luo Y, Liu J, Zhang L, Wu J, Li H, et al. Chemical study of fused ring tetrazine derivatives as possible high energy density materials (HEDMs). Journal of Molecular Modeling 2021;27(9):267. http://dx.doi.org/10.1007/s00894-021-04880-4.

[2] Politzer P, Martinez J, Murray JS, Concha MC, Toro-Labbé A. An electrostatic interaction correction for improved crystal density prediction. Molecular Physics 2009;107(19):2095-101. http://dx.doi.org/10.1080/00268970903156306.

[3] Bader RFW, Carroll MT, Cheeseman JR, Chang C. Properties of atoms in molecules: atomic volumes. Journal of the American Chemical Society 2002;109(26):7968-79. http://dx.doi.org/10.1021/ja00260a006.

[4] Lu T, Chen F. Multiwfn: A multifunctional wavefunction analyzer. Journal of Computational Chemistry 2011;33(5):580-92. http://dx.doi.org/10.1002/jcc.22885.

[5] Lu T. A comprehensive electron wavefunction analysis toolbox for chemists, Multiwfn. The Journal of Chemical Physics 2024;161(8):082503. http://dx.doi.org/10.1063/5.0216272.

[6] Thompson AP, Aktulga HM, Berger R, Bolintineanu DS, Brown WM, Crozier PS, et al. LAMMPS - a flexible simulation tool for particle-based materials modeling at the atomic, meso, and continuum scales. Computer Physics Communications 2022;271. http://dx.doi.org/10.1016/j.cpc.2021.108171.

[7] Sun H. Ab initio calculations and force field development for computer simulation of polysilanes. Macromolecules 2002;28(3):701-12. http://dx.doi.org/10.1021/ma00107a006.

[8] Sun H. COMPASS: An ab Initio Force-Field Optimized for Condensed-Phase ApplicationsOverview with Details on Alkane and Benzene Compounds. The Journal of Physical Chemistry B 1998;102(38):7338-64. http://dx.doi.org/10.1021/jp980939v.

[9] Wang S, Cui Z, Yu C, Tan T. Computational Assessment of the Molecular Structure and Properties for High Energy Density Fuel. The Journal of Physical Chemistry A 2020;124(33):6660-6. http://dx.doi.org/10.1021/acs.jpca.9b11193.

[10] Manring CA, Hawari AI. Assessment of thermal neutron scattering in a heavy paraffinic molecular material. Annals of Nuclear Energy 2019;128:140-7. http://dx.doi.org/10.1016/j.anucene.2018.12.042.

[11] Lu T, Chen Q. Shermo: A general code for calculating molecular thermochemistry properties. Computational and Theoretical Chemistry 2021;1200:113249. http://dx.doi.org/10.1016/j.comptc.2021.113249.

[12] Savos'kin MV, Kapkan LM, Vaiman GE, Vdovichenko AN, Gorkunenko OA, Yaroshenko AP, et al. New approaches to the development of high-performance hydrocarbon propellants. Russian Journal of Applied Chemistry 2007;80(1):31-7. http://dx.doi.org/10.1134/s1070427207010065.

[13] Osmont A, Gökalp I, Catoire L. Evaluating Missile Fuels. Propellants, Explosives, Pyrotechnics 2006;31(5):343-54. http://dx.doi.org/10.1002/prep.200600043.